NANO LETTERS

2009
Vol. 9, No. 5
1798-1805

Gastrin Releasing Protein Receptor Specific Gold Nanorods: Breast and Prostate Tumor Avid Nanovectors for Molecular Imaging

Nripen Chanda, Ravi Shukla, Kattesh V. Katti,* and Raghuraman Kannan*

Department of Radiology, University of Missouri—Columbia, Columbia, Missouri 65212

Received December 9, 2008; Revised Manuscript Received February 17, 2009

ABSTRACT

Gastrin releasing protein receptor specific bombesin (BBN) peptide−gold nanoconjugates were successfully synthesized using gold nanorods and dithiolated peptide. The gold nanorod−bombesin (GNR−BBN) conjugates showed extraordinary in vitro stabilities against various biomolecules including NaCl, cysteine, histidine, bovine serum albumin, human serum albumin, and dithiothreitol. Quantitative measurements on the binding affinity (IC_{50}) of GNR−BBN conjugates toward prostate and breast tumor cells were evaluated. The IC_{50} values establish that GNR−BBN conjugates have strong affinity toward the gastrin releasing peptide receptors on both the tumors. Detailed cellular interaction studies of GNR−BBN conjugates revealed that nanorods internalize via a receptor-mediated endocytosis pathway. The receptor specific interactions of GNR−BBN conjugates provide realistic opportunities in the design and development of in vivo molecular imaging and therapy agents for cancer.

Nanoparticles, due to their smaller sizes and associated unique properties, provide unprecedented opportunities to interrogate cellular and molecular processes with realistic clinical applications.[1−10] Specific types of nanoparticles are being utilized as drug delivery vehicles, cellular biomarkers, and cancer imaging and therapy agents.[1−10] The multifaceted applications of nanoparticles are the direct result of their ability to deliver high payloads of drugs or biomarkers to the desired sites within the body.[1−10] Design and development of tumor-specific nanoparticles could significantly amplify the delivering capacity to a specific target of interest, without affecting healthy cells.[1−10] The target specificity in nanoparticles could be imparted by tagging with certain biovectors, which navigate them to desired organ or site under in vivo conditions. The most commonly used target vectors are monoclonal antibodies and receptor-specific peptides.[11−13] Although, both biomolecules have shown high targeting abilities, the (in vivo) transport properties of monoclonal antibodies and peptides differ drastically. Monoclonal antibodies, due to their larger sizes, show poor in vivo mobility resulting in time delayed and reduced uptake over the desired target. Moreover, monoclonal antibodies are highly immunogenic, which lead to harmful side effects. In sharp contrast, peptides being smaller in size bring various advantages, namely, rapid blood clearance, ease in penetration of tumor vascular endothelium, increased diffusion rates in tissue, and low immunogenicity. Receptors for peptides are highly expressed on a variety of neoplastic and non-neoplastic cells.[14,15] Furthermore, receptor targeting peptides have shown a high level of internalization within the tumor cells via receptor-mediated endocytosis.[16] The ability to internalize probes within tumor cells is important for delivering maximum payloads to tumor cells.[14−16] These attractive physical properties coupled with their smaller size make peptides ideal candidates for developing new target-specific nanoparticles. Therefore, we have designed and developed peptide conjugated nanoparticles that may circumvent some of the currently encountered problems.

Nanoparticles of gold continue to play pivotal roles in the design and development of tumor imaging and therapy agents.[1−13] In particular, gold nanorods (GNRs) have attracted much interest because of their unique photophysical properties, which make them ideal candidates for both tumor imaging and therapeutic applications.[11,17−25] Recent studies are focused on utilizing GNRs as contrast agents for photoacoustic tomography. Indeed, Motamedi and co-workers have shown that engineered gold nanorods, under in vivo conditions, exhibit significant optoacoustic contrast and increase the diagnostic power of optoacoustic imaging modality.[21] Gold nanorods attached with deltorphin, a ligand

* Corresponding authors: tel, 573-8825676; fax, 573-8845679; e-mail, kattik@health.missouri.edu and kannanr@health.missouri.edu.

10.1021/nl8037147 CCC: $40.75
Published on Web 04/07/2009

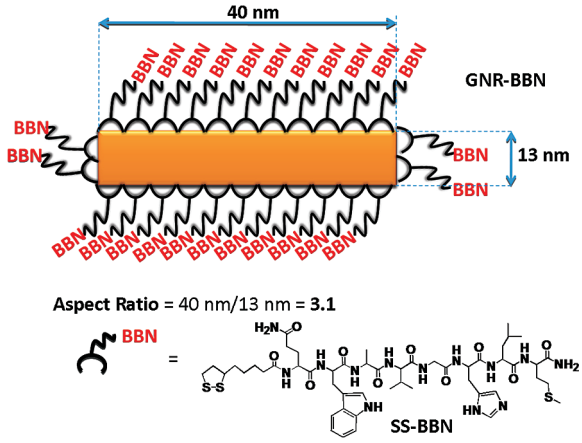

Figure 1. General structure of GNR−BBN conjugates.

with high affinity toward delta opioid receptor, have shown selective absorption toward human colon carcinoma cells, establishing the fact they can serve as contrast agents for molecular imaging.[26] On the therapy front, El-Sayed and co-workers have utilized the plasmon absorption of gold nanorods, in photothermal therapy, as an effective tool against cancer cells.[3] Oyelere et al. demonstrated that peptide-coated gold nanorods can be used as nuclear targeting agents for potential in vivo imaging applications.[27] These literature examples suggest that gold nanorods possess the potential to serve as theranostics, wherein a singular agent can serve as both diagnostic and therapeutic. The theranostic capability of gold nanorods could be realized only when GNRs are selectively localized at tumor sites. The selective delivery of GNRs to tumoral region can be achieved by attaching a target-specific vector. In this context, our studies are focused on utilizing bombesin peptide as a target vector for conjugation with gold nanorods. We hypothesized that bombesin (BBN) peptide can act as a vehicle to deliver gold nanorods specifically to tumor cells. The general structure of gold nanorod−bombesin peptide (GNR−BBN) conjugate is shown in Figure 1.

The 14 amino acid peptide bombesin isolated from the skin of the amphibian *Bombina* and related gastrin-releasing peptides (GRP) exhibit an enhanced response in a variety of tumor tissues, e.g., small cell lung, prostate, breast, and colon cancer.[28−31] BBN functions as potent autocrine or paracrine growth factors for cells.[28−31] In the past decade, a wealth of information was generated on BBN/receptor expression and physiological information. BBN shows high affinity towards GRP receptor subtype BB2. GRP receptors are overexpressed in many cancers, including prostate, breast, and small cell lung cancer.[28−31] Analogues of bombesin with modified structures exhibited a similar or even higher affinity for these receptors.[28−31] Synthetic peptides can be readily generated through automated solid phase techniques. For our studies, we have synthesized and utilized truncated bombesin analogue (BBN) as a vehicle to target GRP receptors (Figure 1).

The main objective of our investigation is to examine whether the synthetic bombesin peptide conjugated gold nanorods can preferentially locate GRP receptors, which are overexpressed in prostate and breast tumor cells for subsequent applications as theranostic agents. As part of our overall goal on developing target-specific gold nanoparticles for treatment of cancers,[32−34] we carried out a systematic investigation on the design and development of targeted gold nanorods by conjugating with GRP-receptor avid bombesin peptide. Our studies, for the first time to our knowledge, establish that GNR−BBN conjugates have very high binding affinity toward GRP receptors in cancer cells and internalize via receptor-mediated endocytosis pathway. The results reported in this letter include (i) synthesis and characterization of gold nanorod−bombesin (GNR−BBN) conjugates, (ii) in vitro stability studies of GNR−BBN conjugates toward various biomolecules, (iii) evaluation of binding affinity (IC_{50}) values of GNR−BBN conjugates toward GRP receptors overexpressed in prostate and breast tumor cells, and (iv) evaluation of internalization mechanism of GNR−BBN conjugates in cells.

Production of GNR−Bombesin Bioconjugates. Synthetic analogues of bombesin have been proven to show a similar binding affinity as the nascent bombesin peptide with GRP receptors.[28−31] On the basis of our extensive previous studies, we have selected the peptide sequence shown in Scheme 1 for conjugation with gold nanorods. In the present study, GNRs of aspect ratio 3.1, capped with surfactant cetyltrimethylammonium bromide (CTAB), have been employed. These GNRs show a strong absorption band at 725 nm due to longitudinal oscillations of electrons. The conventional method of surface conjugation of biomolecules to GNRs involved replacement of capping CTAB ligands with monodentate thiolated biomolecules to form Au−S bonds. Although the conjugation is very effective, it suffers a major drawback as the Au−S bond undergoes an irreversible oxidation and consequent elimination under biological conditions. Elimination of these surface bound ligands from nanoparticles leads to instant destabilization of these conjugates to form macroaggregates. In order to circumvent this problem, we have utilized a cyclic dithio moiety, thioctic acid (TA), as a linker between GNR and bombesin peptide (Figure 1 and Scheme 1). This dithio moiety chelates with gold atoms on the surface of GNRs leading to a more stable cyclic structure. Indeed, TA conjugated gold nanospheres (AuNPs) have shown extraordinary stability when compared with that of monothiol bound gold nanoconjugates.[35−44] For example, Abad et al. have used 3 nm TA−AuNPs as highly stable scaffolds for conjugation with cobalt(II) complex for subsequent interaction with histidine-tagged protein,[35] and TA−AuNPs have also been reported as a biological probe by attaching with electroluminescent luminol.[36] Mirkin and Graham have independently established the high stability attained by AuNPs upon conjugation with TA−oligonucleotides.[37,38] Recently, Li and co-workers have demonstrated the high in vitro and in vivo stabilities of AuNPs coated with TA−PEG than that of AuNPs conjugated with monothiol-PEG.[44] These literature examples suggest that TA can serve as ideal ligands for covalent binding of AuNPs with antibodies or peptides for in vivo imaging and therapy applications.[44] Another reason for the choice of disulfide as

Scheme 1. Synthesis of GNR−BBN Conjugates (**2a**−**2c**) Followed by Treatment with 10% NaCl[a]

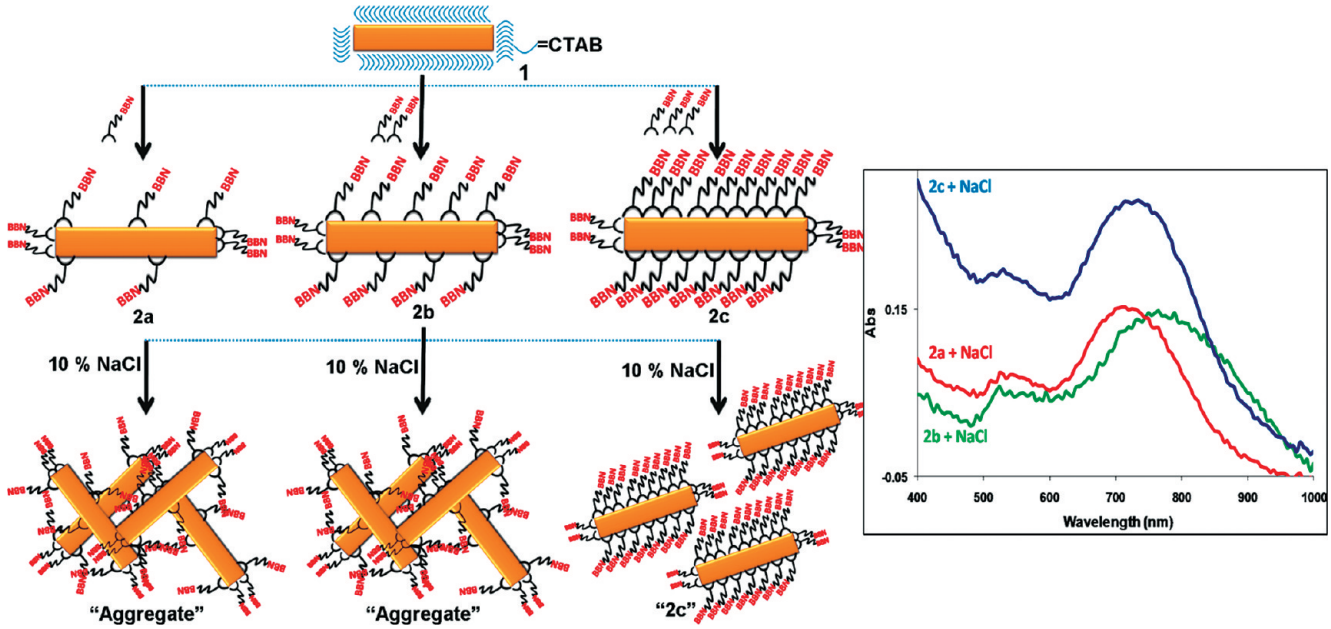

[a] Plasmon resonance bands of **2a** and **2b** show broadening after mixing with 10% NaCl, whereas the plasmon band of **2c** remains unaltered.

a starting material is based on the fact that this moiety is stable under peptidic reaction conditions. In sharp contrast, free thiols on peptidic reaction conditions form disulfides to yield mixtures. This complication poses additional problems during the synthesis of thiols containing peptides. In this study, we have synthesized dithioctic acid conjugate of bombesin peptide using standard Fmoc methodology using solid phase support. We chose commercially available thioctic acid as a ligand to covalently link gold and bombesin peptide. Thioctic acid contains two functional groups, a disulfide and a carboxylic group. The carboxyl group of thioctic acid was attached with N-terminal of bombesin peptide via conventional solid-phase peptide synthesis to yield thioctic−bombesin conjugate (SS−BBN, Figure 1). The dithiobombesin (SS−BBN) was purified by standard HPLC methods. The SS−BBN peptide is remarkably stable at 4 °C and shows no detectable decomposition even after 1 year. The disulfide group in SS−BBN was utilized to conjugate with GNRs.

The GNR−bombesin conjugates were synthesized by stirring CTAB−GNRs (**1**) with SS−BBN peptide (Scheme 1). In order to coat different amounts of SS−BBN over the surface of GNRs, we varied the GNR-to-SS−BBN ratio (1: SS−BBN = 1:1, 1:2, and 1:3; **2a**, **2b**, and **2c**, respectively). Typical experimental procedure involves dissolution of **1** and SS−BBN in water−methanol mixture and stirring for 20 h. From the resulting mixture, GNR−BBN conjugates were removed by centrifuging the solution at 8000*g*. The residue was washed several times with water and methanol to remove CTAB molecules and unreacted SS−BBN peptide. The UV−visible spectra of GNR−BBN conjugates show a slight change in the plasmon absorption band from that of **1** (Figure 2a). The examination of GNR−BBN conjugates under transmission electron microscopy revealed distinct rod-shaped structures with no sign of aggregation or change in shape, with an average aspect ratio of 3.1; this size is comparable to that of **1** (Figure 2b). We believe the coexistence of both disulfide and ring structure in SS−BBN provides synergistic advantages in rigid binding with gold nanoparticles.

We examined the degree of bombesin coating in **2a**, **2b**, and **2c** by treating the aqueous solution of the conjugates with 10% NaCl solution, followed by monitoring the plasmon resonance band. If the coating of SS−BBN peptide over GNRs is insufficient, then the surface gold atoms will be exposed to ionic NaCl solution. This event triggers aggregation of the nanoparticles resulting in the broadening of absorption band. Of the three conjugates, **2a** and **2b** show broadening of the longitudinal plasmon absorption band after mixing with 10% NaCl. On the other hand, the UV−visible plasmon resonance band of **2c** remains unaltered after treatment with 10% NaCl. This observation unequivocally demonstrates that in **2c** the surface atoms are covered by SS−BBN peptides. In order to ascertain the conjugation of SS−BBN over GNR, we measured the zeta potential (ζ-potential) of GNR−CTAB and GNR−BBN (**2c**) conjugates. The ζ-potential of CTAB-coated gold nanorods is +48.0 mV because of the presence of cationic CTAB on the surface. The ζ-potential of **2c** is −32.0 mV. The resulting negative charge in GNR−BBN conjugate can be attributed to negative surface charge in "naked" gold nanorods.

In Vitro Stability Studies of GNR−BBN Conjugate. The in vitro stabilities of GNR−BBN conjugates were evaluated by treating aqueous solutions of nanoconjugates with various biologically relevant molecules for 12 h, followed by monitoring the plasmon resonance band (Figure 3). The molecules that are commonly encountered under in vivo conditions include NaCl, HSA, cysteine, histidine, and biological buffer additives such as dithiothreitol (DTT). These molecules possess the ability to dislodge thiolated ligands from gold−thiol nanoconjugates. The removal of thiolated ligands would lead to aggregation of gold nano-

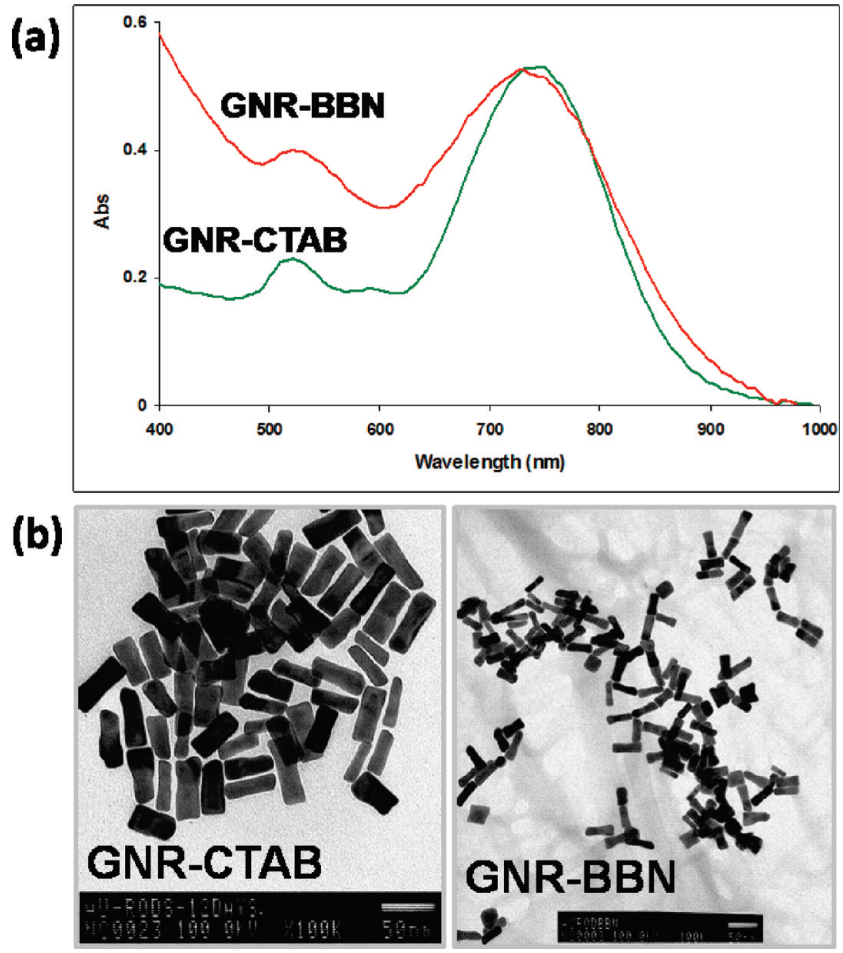

Figure 2. GNR−CTAB and GNR−BBN conjugates: (a) UV−vis spectra; (b) transmission electron microscopy images.

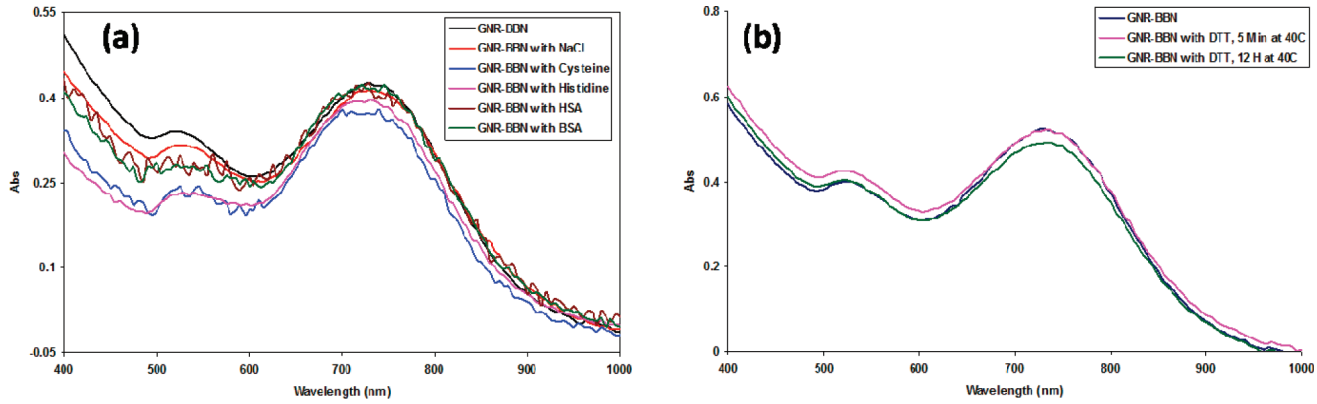

Figure 3. In vitro stability studies of GNR−BBN conjugate **2c** in various biological media: (a) UV−visible spectra of **2c** after 12 h of treatment with 0.9% NaCl, cysteine, histidine, HSA, or BSA; (b) UV−visible spectra of **2c** in various time points after treatment with DTT at 40 °C.

particles, resulting in broadening of the plasmon resonance band. Therefore, this study may provide greater understanding on the in vivo stability of the conjugates. The aqueous solutions of **2c** were mixed with 0.9% NaCl, 0.5% cysteine, 0.2 M histidine, 0.5% HSA, or 0.5% BSA solutions and stirred for 12 h, and the UV−visible spectra of the resulting solutions were recorded (Figure 3a). It is important to recognize that the plasmon absorption bands of **2c** did not show any change in peak width or shape (Figure 3).

The examination of thiolated gold nanoconjugates in the presence of DTT is emerging as a standard test in establishing in vitro stability.[37,38] For example, gold−monothiol conjugates upon treatment with DTT releases more than 70% of the thiols from the gold surface, within 12 h of treatment. The rate of release of bound ligands from the surface serves as a direct measure on the stability of the conjugate under biological conditions. In the case of gold−dithiol conjugates, the release of dithiol ligand from the surface of gold is very

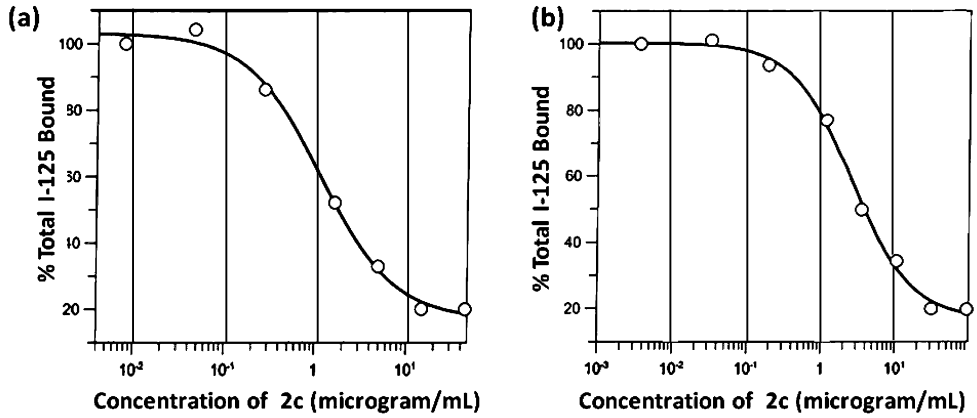

Figure 4. IC_{50} values of **2c** against ^{125}I-BBN in GRP receptors expressing (a) prostate tumor PC-3 cells and (b) breast tumor T-47D cells.

limited. This in vitro stability can be attributed to strongly chelating cyclic dithiols.

In order to unambiguously establish the stability of conjugate **2c**, we have monitored the aggregation characteristics for 12 h after treatment with 10 mM DTT at 40 °C. Typically, GNR−BBN conjugate **2c** was treated with 10 mM DTT solution and heated at 40 °C for 12 h. Release of bound thioctic acid−bombesin peptide from GNR−BBN is expected to shift the plasmon bands of gold nanorods. Monitoring the plasmon band provides the opportunity to comment on the in vitro stability of **2c**. The UV−visible spectra of **2c** after treatment with DTT were monitored for a period of 12 h (Figure 3b). The plasmon bands remained unaltered throughout the period suggesting extraordinary in vitro stability of **2c**.

These data clearly confirm that **2c** is highly stable in solutions of NaCl, cysteine, histidine, HSA, BSA, or DTT. It is conceivable that the chelate formed from the disulfide ring structure contained within the SS−BBN backbone with gold atoms provides extraordinary in vitro stability. These findings provide solid corroboration that bonds between the dithio moiety and gold atoms in GNR−BBN conjugates are highly stable under in vivo conditions for further use in imaging applications.

In Vitro Competitive Cell Binding Affinity Assays of GNR−BBN Conjugate. Recently, Chan and co-workers have evaluated the quantitative uptake of herceptin-coated gold nanoparticles in ErbB2 overexpressing human breast cancer SK-BR-3 cells using fluorescent imaging.[4] In the present report, we performed detailed competitive cell binding affinity assays to evaluate IC_{50} values of conjugates **2a**−**2c** in prostate (PC-3) and breast (T-47D) cancer cells. Both PC-3 and T-47D cells exhibit a large number of GRP receptors on the surface of the cells. The IC_{50} values of GNR−BBN conjugates were determined against the radioactive bombesin analogue ^{125}I-Tyr^4 BBN, which serves as a GRP receptor specific peptide. In order to evaluate the IC_{50} values, the radioactive ^{125}I-Tyr^4 BBN was co-incubated with increasing concentrations of GNR−BBN conjugates in PC-3 and T-47D cells. After the incubation period, cells were washed several times and cell bound radioactivity was measured. The IC_{50} values were determined by plotting the cell-bound radioactivity of ^{125}I-Tyr^4 BBN versus the concentrations of GNR−BBN conjugates (Figure 4). Table 1 summarizes the IC_{50} values of GNR−BBN conjugates **2a**−**2c**. The IC_{50} values for the conjugates were reported in micrograms, as the molecular weights of the conjugates cannot be accurately determined. It is evident from the data that the IC_{50} values or cell binding affinity of conjugates depend on the degree of BBN peptide coating over gold nanorods. For instance, conjugate **2c**, which has a greater number of bombesin peptides on the surface of GNR, exhibits a lower IC_{50} value (or higher cell-binding affinity) when compared with other conjugates. The IC_{50} values of GNR−BBN conjugates are comparable for both PC-3 and T-47D cells. This study confirms that GNR−BBN conjugates show high affinity toward GRP receptors overexpressed in prostate cancer (PC-3 cell line) and breast cancer (T-47D cell line).

Table 1. Quantitative Measure of Binding Affinity (IC_{50}) of GNR−BBN Conjugates toward GRP Receptors

	IC-50 value (μg/mL)	
conjugate	PC-3 (prostate tumor cells)	T-47D (breast tumor cells)
2a	11.89	7.57
2b	4.91	3.52
2c	2.62	2.12

Interaction of GNR−BBN with PC-3 and T-47D Cancer Cells. The cellular localizations of GNR−BBN nanoconjugates in PC-3 and T-47D cells, which overexpress GRP receptors, were evaluated using dark field optical microscopy and transmission electron microscope image analysis. It is widely accepted that the internalization of nanoparticles strongly depends on their physical characteristics including size, shape, and charge. Recently, DeSimone and co-workers have demonstrated that nanoparticles with either larger size or negative zeta potential exhibit no cellular internalizations.[45] In that study, authors concluded that investigating the internalization of nanoparticles bearing negative zeta potential and conjugated with receptor-stimulating ligand would be interesting. In order to deliver negatively charged DNA inside the cells, researchers have utilized ammonium ions as vectors; the ammonium cation interacts effectively with a negatively charged cell membrane,

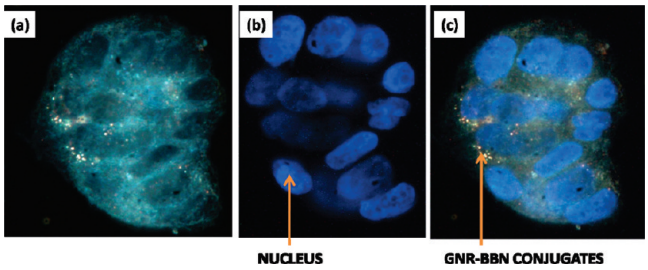

Figure 5. (a) Dark-field image of breast tumor cells (T-47D) after treatment with GNR−BBN conjugate **2c**. (b) Fluorescence image of nucleus of breast tumor cells. (c) Dark-field and fluorescence overlap images indicating that GNRs are not localized in nuclei.

triggering charge-mediated endocytosis. It is important to note here that GNR−BBN conjugate **2c** has a negative ζ-potential of −32.0 mV. As a negative zeta potential candidate, **2c** is expected to have very minimal or no interaction with negatively charged cell surface. In addition, **2c** does not have any positively charged ions on the surface, thus possesses no ability to trigger charge-mediated endocytosis. These results indirectly suggest that internalization of **2c** would be possible only by means of specific internalization events. This behavior is also expected because the bombesin sequence chosen in the present study has agonist properties, which means they have specific receptor (in this case, GRP receptor) triggering characteristics to internalize within the cells. Our investigations focused on two important aspects and they are as follows: (i) location of **2c** within the cellular matrices, and (ii) understanding the mechanism of internalization of conjugate **2c** in GRP receptors expressing cancer cells.

As a first step, we recorded dark field light-scattering images of T-47D cells after incubation with **2c** (Figure 5). The bright light scattering in the dark field image is due to the presence of a unique longitudinal surface plasmon oscillation which has a resonance frequency within the near-IR region of the optical spectrum. The images confirm that nanoparticles, as expected, have not entered into the nucleus. Our detailed investigations used transmission electron microscopy (TEM) images and are discussed in the following sections.

Receptor-Mediated Endocytosis. The mechanism of either phagocytosis or receptor-mediated endocytosis is considered the "holy grail" of internalization of nanoparticles within cells. The widely accepted internalization mechanisms for nanoparticles are via phagocytosis or receptor-mediated endocytosis. In order to evaluate the internalization mechanism, we have carried out a detailed examination of TEM images of cancer cells treated with **2c**. TEM images, shown in Figure 6, strongly suggest that the internalization occurs via receptor-mediated endocytosis, and phagocytosis is not observed. It is important to note that the cellular membrane did not show the formation of phagocytic cups, which are usually present in the cell wall if the phagocytosis has occurred. In addition, the conjugates of **2c** were not found in endosomes but were present in cytosol (see Figure 6). It is commonly observed that phagocytosed gold nanoparticles form a dense mass of aggregated nanoparticles, secluded

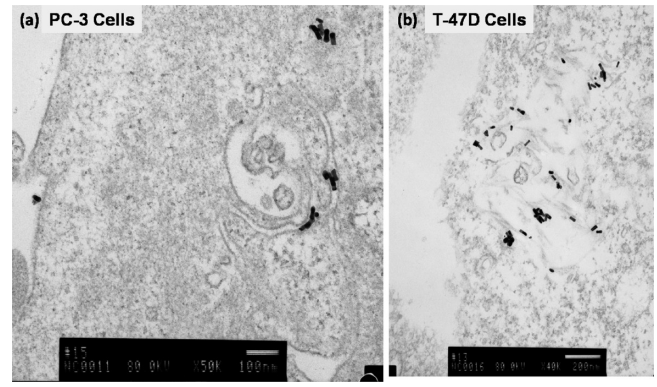

Figure 6. TEM images of cells after treatment with GNR−BBN conjugate **2c**: (a) PC-3 cells; (b) T-47D. GNR−BBN conjugates are present in cytosol and show no formation of endosomes.

from the rest of the cells in endosomal vesciles. Recently, Brust and co-workers reported their results on the interaction of citrate-stabilized nanoparticles and CALNN-coated nanoparticles with HeLa cells; they observed the formation of densely packed aggregated nanoparticles in endosomes.[46] Further, these studies have unequivocally demonstrated the delivery of nanoparticles conjugated with cell penetrating peptides selectively to cytosol without any uptake within the endosomes.[46] In sharp contrast, the PEG-ylated nanoparticles, which are devoid of any targeting vector, did not show any sign of internalization.[46] Therefore, we can infer that nanoparticles coated with receptor specific peptides can be endocytosed predominantly via non-phagocytosis pathway. The generalized view is that nanoparticles that are susceptible for interaction with serum proteins, such as citrate-stabilized nanoparticles, tend to be prone for phagocytosis. On the other hand, if the nanoparticles are stable toward serum proteins (for example, PEG-ylated nanoparticles) which lack cell targeting capabilities, they will not be internalized into the cells. In the light of these findings, it is expected that nanoconjugate **2c**, which resists interaction with serum protein, should not undergo phagocytosis. However, the targeting vector bombesin in **2c** is anticipated to stimulate GRP receptors in the cellular surface, thus providing opportunity to penetrate into cells. In order to corroborate that the internalization of GNR−BBN conjugates in PC-3 and T-47D occurs via receptor-mediated endocytosis pathway, our studies focused on understanding the interaction of GNR−BBN conjugates with cells which lack GRP receptors. For this experiment, we used NIH-3T3 cells, which do not express GRP receptors.[47] GNR−BBN conjugates **2c** were incubated with NIH-3T3 cells and monitored through TEM images. As shown in Figure 7, significantly fewer GNRs internalize in NIH-3T3 cells. Most importantly, the internalized GNRs were present in endosomes and not in cytosol. Our experimental results, as discussed above, have clearly shown the uptake of bombesin-based nanoparticles in cytosol when incubated with T-47D and PC-3 cells, both of which are known to overexpress GRP receptors. These observations corroborate that the mode of internalization of GNRs in NIH-3T3 cells is predominantly via phagocytosis, whereas

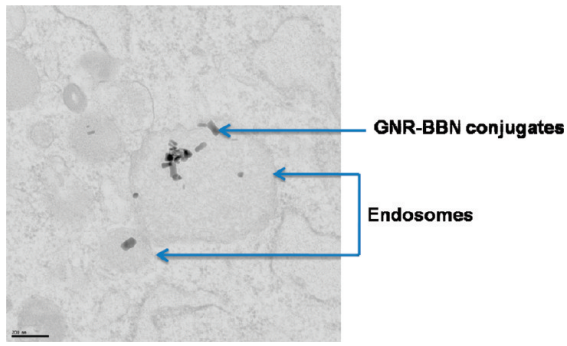

Figure 7. TEM image of NIH-3T3 cells after treatment with GNR−BBN conjugate **2c**.

internalization within PC-3 and T-47D proceeded via receptor-mediated endocytosis pathway.

In summary, we have developed a novel strategy for the synthesis of gold nanorod−bombesin (GNR−BBN) conjugates. The degree of coating of bombesin peptides over the surface of GNRs can be tuned by adjusting the GNR-to-SS−BBN ratio. Our detailed investigations confirm that GNR−BBN conjugates show very high affinity toward prostate and breast cancers, which overexpress GRP receptors. The quantitative measure on the affinity of GNR−BBN conjugates to various GRP-receptor positive tumors has been evaluated. The internalization of GNR−BBN conjugates via receptor-mediated endocytosis in GRP-receptor positive cells was confirmed by TEM image analysis and dark field microscopy analysis. Detailed investigations on the internalization mechanism of GNR−BBN have provided new insights on the conjugates and confirm a receptor-mediated endocytosis mechanism in GRP-receptor positive cells. The selective cancer-targeting capabilities of GNR−BBN conjugates and the associated in vitro stabilities provide unprecedented opportunities for the utilization of GNR−BBN vectors in molecular imaging and therapy of cancer.

Acknowledgment. Dark-field images are courtesy of CytoViva Inc. Authors thank Dr. Gary L. Sieckman and Dr. Timothy J. Hoffman, H. S. Truman Memorial Veterans Hospital, Columbia, for estimation of IC_{50} values of GNR-BBN conjugates. This work has been supported by the National Institutes of Health/National Cancer Institute under the Cancer Nanotechnology Platform program and Nanoscience and Nanotechnology program (Grant Numbers 5R01CA119412-04 and 1R21CA128460-02).

Supporting Information Available: (i) Synthesis and characterization of gold nanorods, (ii) synthesis and purification of thioctic acid−bombesin (SS−BBN) conjugate, (iii) synthesis and characterization of gold nanorod−bombesin conjugates (GNR−BBN), (v) in vitro stability studies of GNR−BBN conjugates, and (vi) cellular internalization studies of GNR−BBN conjugates. This material is available free of charge via the Internet at http://pubs.acs.org.

References

(1) Jain, P. K.; Huang, X.; El-Sayed, I. H.; El-Sayed, M. A. *Acc. Chem. Res.* **2008**, *41*, 1578–1586.
(2) Rabin, O.; Manuel Perez, J.; Grimm, J.; Wojtkiewicz, G.; Weissleder, R. *Nat. Mater.* **2006**, *5*, 118–122.
(3) Huang, X.; El-Sayed, I. H.; Qian, W.; El-Sayed, M. A. *J. Am. Chem. Soc.* **2006**, *128*, 2115–20.
(4) Jiang, W.; Kim, B. Y.; Rutka, J. T.; Chan, W. C. *Nat. Nanotechnol.* **2008**, *3*, 145–50.
(5) Skala, M. C.; Crow, M. J.; Wax, A.; Izatt, J. A. *Nano Lett.* **2008**, *8*, 3461–7.
(6) Popovtzer, R.; Agrawal, A.; Kotov, N. A.; Popovtzer, A.; Balter, J.; Carey, T. E.; Kopelman, R. *Nano Lett.* **2008**, *8*, 4593–4596.
(7) Loo, C.; Lowery, A.; Halas, N.; West, J.; Drezek, R. *Nano Lett.* **2005**, *5*, 709–11.
(8) Kumar, S.; Harrison, N.; Richards-Kortum, R.; Sokolov, K. *Nano Lett.* **2007**, *7*, 1338–43.
(9) Chithrani, B. D.; Ghazani, A. A.; Chan, W. C. *Nano Lett.* **2006**, *6*, 662–8.
(10) Chithrani, B. D.; Chan, W. C. *Nano Lett.* **2007**, *7*, 1542–50.
(11) Pissuwan, D.; Valenzuela, S. M.; Miller, C. M.; Cortie, M. B. *Nano Lett.* **2007**, *7*, 3808–12.
(12) Souza, G. R.; Christianson, D. R.; Staquicini, F. I.; Ozawa, M. G.; Snyder, E. Y.; Sidman, R. L.; Miller, J. H.; Arap, W.; Pasqualini, R. *Proc. Natl. Acad. Sci. U.S.A.* **2006**, *103*, 1215–20.
(13) Qian, X.; Peng, X. H.; Ansari, D. O.; Yin-Goen, Q.; Chen, G. Z.; Shin, D. M.; Yang, L.; Young, A. N.; Wang, M. D.; Nie, S. *Nat. Biotechnol.* **2008**, *26*, 83–90.
(14) Eidne, K. A.; Flanagan, C. A.; Millar, R. P. *Science* **1985**, *229*, 989–991.
(15) Reubi, J. C.; Gugger, M.; Waser, B.; Schaer, J. C. *Cancer Res.* **2001**, *61*, 4636–4641.
(16) Alam, M. R.; Dixit, V.; Kang, H.; Li, Z. B.; Chen, X.; Trejo, J.; Fisher, M.; Juliano, R. L. *Nucleic Acids Res.* **2008**, *36*, 2764–2776.
(17) Murphy, C. J.; Gole, A. M.; Stone, J. W.; Sisco, P. N.; Alkilany, A. M.; Goldsmith, E. C.; Baxter, S. C. *Acc. Chem. Res.* **2008**, *41*, 1721–1730.
(18) Caswell, K. K.; Wilson, J. N.; Bunz, U. H.; Murphy, C. J. *J. Am. Chem. Soc.* **2003**, *125*, 13914–13915.
(19) Chen, C. C.; Lin, Y. P.; Wang, C. W.; Tzeng, H. C.; Wu, C. H.; Chen, Y. C.; Chen, C. P.; Chen, L. C.; Wu, Y. C. *J. Am. Chem. Soc.* **2006**, *128*, 3709–3715.
(20) Durr, N. J.; Larson, T.; Smith, D. K.; Korgel, B. A.; Sokolov, K.; Ben-Yakar, A. *Nano Lett.* **2007**, *7*, 941–945.
(21) Eghtedari, M.; Oraevsky, A.; Copland, J. A.; Kotov, N. A.; Conjusteau, A.; Motamedi, M. *Nano Lett.* **2007**, *7*, 1914–1918.
(22) El-Sayed, I. H.; Huang, X.; El-Sayed, M. A. *Nano Lett.* **2005**, *5*, 829–834.
(23) Everts, M.; Saini, V.; Leddon, J. L.; Kok, R. J.; Stoff-Khalili, M.; Preuss, M. A.; Millican, C. L.; Perkins, G.; Brown, J. M.; Bagaria, H.; Nikles, D. E.; Johnson, D. T.; Zharov, V. P.; Curiel, D. T. *Nano Lett.* **2006**, *6*, 587–591.
(24) Huang, X.; El-Sayed, I. H.; Qian, W.; El-Sayed, M. A. *Nano Lett.* **2007**, *7*, 1591–1597.
(25) Skrabalak, S. E.; Chen, J.; Sun, Y.; Lu, X.; Au, L.; Cobley, C. M.; Xia, Y. *Acc. Chem. Res.* **2008**, *41*, 1587–1595.
(26) Black, K. C.; Kirkpatrick, N. D.; Troutman, T. S.; Xu, L.; Vagner, J.; Gillies, R. J.; Barton, J. K.; Utzinger, U.; Romanowski, M. *Mol. Imaging* **2008**, *7*, 50–57.
(27) Oyelere, A. K.; Chen, P. C.; Huang, X.; El-Sayed, I. H.; El-Sayed, M. A. *Bioconjugate Chem.* **2007**, *18*, 1490.
(28) Maina, T.; Nock, B.; Mather, S. *Cancer Imaging* **2006**, *6*, 153–157.
(29) Abd-Elgaliel, W. R.; Gallazzi, F.; Garrison, J. C.; Rold, T. L.; Sieckman, G. L.; Figueroa, S. D.; Hoffman, T. J.; Lever, S. Z. *Bioconjugate Chem.* **2008**, *19*, 2040–2048.
(30) Biddlecombe, G. B.; Rogers, B. E.; de Visser, M.; Parry, J. J.; de Jong, M.; Erion, J. L.; Lewis, J. S. *Bioconjugate Chem.* **2007**, *18*, 724–730.
(31) Lin, K. S.; Luu, A.; Baidoo, K. E.; Hashemzadeh-Gargari, H.; Chen, M. K.; Brenneman, K.; Pili, R.; Pomper, M.; Carducci, M. A.; Wagner, H. N., Jr. *Bioconjugate Chem.* **2005**, *16*, 43–50.
(32) Shukla, R.; Nune, S. K.; Chanda, N.; Katti, K.; Mekapothula, S.; Kulkarni, R. R.; Welshons, W. V.; Kannan, R.; Katti, K. V. *Small* **2008**, *4*, 1425–1436 (Appeared as Editors choice in *Science*, 2008.).
(33) Kattumuri, V.; Katti, K.; Bhaskaran, S.; Boote, E. J.; Casteel, S. W.; Fent, G. M.; Robertson, D. J.; Chandrasekhar, M.; Kannan, R.; Katti, K. V. *Small* **2007**, *3*, 333–341.
(34) Kannan, R.; Rahing, V.; Cutler, C.; Pandrapragada, R.; Katti, K. K.; Kattumuri, V.; Robertson, J. D.; Casteel, S. J.; Jurisson, S.; Smith, C.; Boote, E.; Katti, K. V. *J. Am. Chem. Soc.* **2006**, *128*, 11342–3.

(35) Abad, J. M.; Mertens, S. F. L.; Pita, M.; Fernandez, V. M.; Schiffrin, D. J. *J. Am. Chem. Soc.* **2005**, *127*, 5689–5694.
(36) Roux, S.; Garcia, B.; Bridot, J.−L.; Salom, M.; Marquette, C.; Lemelle, L.; Gillet, P.; Blum, L.; Perriat, P.; Tillement, O. *Langmuir* **2005**, *21*, 2526–2536.
(37) Li, Z.; Jin, R.; Mirkin, C. A.; Letsinger, R. L. *Nucleic Acids Res.* **2002**, *30*, 1558–1562.
(38) Dougan, J. A.; Karlsson, C.; Smith, W. E.; Graham, D. *Nucleic Acids Res.* **2007**, *35*, 3668–3675.
(39) Letsinger, R. L.; Elghanian, R.; Viswanadham, G.; Mirkin, C. A. *Bioconjugate Chem.* **2000**, *11*, 289–291.
(40) Yonezawa, T.; Yasui, K.; Kimizuka, N. *Langmuir* **2001**, *17*, 271–273.
(41) Porter, L. A., Jr.; Ji, D.; Westcott, S. L.; Graupe, M.; Czernuszewicz, R. S.; Halas, N. J.; Lee, T. R. *Langmuir* **1998**, *14*, 7378.
(42) Garcia, B.; Salome, M.; Lemelle, L.; Bridot, J.−L.; Gillet, P.; Perriat, P.; Roux, S.; Tillement, O. *Chem. Commun.* **2005**, *3*, 369–371.
(43) Karamanska, R.; Mukhopadhyay, B.; Russel, D. A.; Field, R. A. *Chem. Commun.* **2005**, *26*, 3334–3336.
(44) Zhang, G.; Yang, Z.; Lu, W.; Zhang, R.; Huang, Q.; Tian, M.; Li, L; Liang, D.; Li, C. *Biomaterials* **2009**, *30*, 1928–1936.
(45) Gratton, S. E.; Ropp, P. A.; Pohlhaus, P. D.; Luft, J. C.; Madden, V. J.; Napier, M. E.; DeSimone, J. M. *Proc. Natl. Acad. Sci. U.S.A.* **2008**, *105*, 11613–11618.
(46) Nativo, P; Prior, I. A.; Brust, M. *ACS Nano* **2008**, *2*, 1639–1644.
(47) Gollan, T. J.; Green, M. R. *J. Virol.* **2002**, *76*, 3564–3569.

NL8037147